Hydrophilicity of a Single Residue within MscL Correlates with Increased Channel Mechanosensitivity

Kenjiro Yoshimura, Ann Batiza, Matt Schroeder, Paul Blount, and Ching Kung
Laboratory of Molecular Biology, University of Wisconsin, Madison, Wisconsin 53706, USA

ABSTRACT Mechanosensitive channel large (MscL) encodes the large conductance mechanosensitive channel of the *Escherichia coli* inner membrane that protects bacteria from lysis upon osmotic shock. To elucidate the molecular mechanism of MscL gating, we have comprehensively substituted Gly^{22} with all other common amino acids. Gly^{22} was highlighted in random mutagenesis screens of *E. coli* MscL (Ou et al., 1998, *Proc. Nat. Acad. Sci. USA*. 95:11471–11475). By analogy to the recently published MscL structure from *Mycobacterium tuberculosis* (Chang et al., 1998, *Science*. 282:2220–2226), Gly^{22} is buried within the constriction that closes the pore. Substituting Gly^{22} with hydrophilic residues decreased the threshold pressure at which channels opened and uncovered an intermediate subconducting state. In contrast, hydrophobic substitutions increased the threshold pressure. Although hydrophobic substitutions had no effect on growth, similar to the effect of an *MscL* deletion, channel hyperactivity caused by hydrophilic substitutions corrrelated with decreased proliferation. These results suggest a model for gating in which Gly^{22} moves from a hydrophobic, and through a hydrophilic, environmment upon transition from the closed to open conformation.

INTRODUCTION

Organisms must respond specifically to a variety of pressure stimuli such as touch, gravity, barometric pressure, turgor, and osmotic changes. It is becoming apparent that pressure stimuli often cause ion channel opening, effectively transducing a particular mechanical stimulus into an electrical or chemical one that the cell can interpret (for reviews, see: French, 1992; Bargmann, 1994; Sackin, 1995; Hamill and McBride, 1996; Kernan, 1997; Sukharev et al., 1997; Sachs and Morris, 1998).

Mechanically gated ion conductances are found in over 30 cell types, including animal tissues exposed to osmotic or cardiovascular deformation (Lansman et al., 1987; Christensen, 1987; Ubl et al., 1988). Such mechanosensitive conductances are also detected in plant, yeast, and bacterial cells (Sukharev et al., 1997); in *Escherichia coli*, such conductances are called MscM, MscS, and MscL—respectively, *M*echano*s*ensitive *c*hannel *M*ini, *S*mall, and *L*arge—conductances (Sukharev et al., 1993; Berrier et al., 1996). MscL, which was the first mechanosensitive channel cloned (Sukharev et al., 1994), forms a mutimeric channel (now thought to be a pentamer) in the inner membrane that is both necessary and sufficient to allow gating by membrane stretch (Berrier et al., 1989; Sukharev et al., 1994; Blount et al., 1996c; Häse et al., 1997; Saint et al., 1998; Sukharev et al., 1999a). Each subunit has only 136 amino acids that generate two α-helical transmembrane domains, a connecting periplasmic loop, and two cytoplasmic domains (Sukharev et al., 1994; Blount et al., 1996b; Arkin et al., 1997), a topology recently supported by the crystallographic structure of the *Mycobacterium tuberculosis* homologue, Tb-MscL (Chang et al., 1998). Sieving and conductance studies show that the channel opens to a large, ~30–40-Å pore (Cruickshank et al., 1997; Sukharev et al., 1999b), which passes a large nanoSiemens current that is relatively nonspecific (Martinac et al., 1987, Sukharev et al., 1993, 1994). Several studies support this channel's role in osmoregulation: 1) *mscL* gain of function (GOF) mutants at K31 that lose potassium upon hypotonic shock can be rescued by osmotically supported medium (Blount et al., 1997); 2) hypotonic shock causes MscL channels to pass solutes, including small proteins such as the 12 kD thioredoxin (Ajouz et al., 1998); and 3) a marine bacterium can be rescued from osmotic lysis by heterologously expressed *E. coli* MscL (Nakamaru et al., 1999). The most compelling evidence shows that cells deprived of both MscL and YggB, which contributes to MscS activity, lyse upon osmotic shock. Loss of either gene alone has no effect (Levina et al., 1999).

Because MscL serves as a model for how a protein changes conformation in response to membrane tension, much research has centered upon determining the molecular basis for its gating. Two studies implicate the lower half of the first transmembrane domain as important in gating. The pentameric Tb-MscL crystallographic structure shows a constriction between Ile^{14} and Val^{21} that is formed by the lower half of all five TM1 helices (Chang et al., 1998). The biological significance of this highly conserved region (Moe

Received for publication 12 April 1999 and in final form28 June 1999.

*The first two authors contributed equally.

Address reprint requests to Ching Kung, Laboratory of Molecular Biology, University of Wisconsin, Madison, WI 53706. Tel.: 608-262-9472; Fax: 608-262-4570; E-mail: ckung@facstaff.wisc.edu.

Dr. Yoshimura's present address is Department of Biological Science, Graduate School of Science, University of Tokyo, Hongo, Tokyo 113-0033, Japan.

Mr. Schroeder's present address is Enzyme Institute, University of Wisconsin, Madison, WI 53706.

Dr. Blount's present address is Department of Physiology, University of Texas, Southwestern Medical Center, Dallas, TX 75235.

0006-3495/99/10/1960/13 $2.00

et al., 1998) was underscored by random mutagenesis of *E. coli* (Ou et al., 1998). In this genetic screen, mutations that resulted in slow or no growth phenotypes were isolated. Although the entire *E. coli* mscL gene was mutagenized, 14 of 18 *mscL* mutants isolated had substitutions in one of the amino acids ranging from positions 13 to 30, which correspond to residues 11 to 28 of Tb-MscL. The most severe growth defects correlated with channels that open with little or no stretch force (Ou et al., 1998). Among this group were numerous mutations in Gly^{22} (Ou et al., 1998), a residue highly conserved among bacteria (Moe et al., 1998). By analogy, the Tb-MscL crystal structure gives us a static snapshot of the closed *E. coli* channel. Given that the open pore of the *E. coli* channel must be huge to account for its ability to conduct bulky solutes (Cruickshank et al., 1997; Ajouz et al., 1998; Sukharev et al., 1999b), and given that the solved structure appears to represent a closed state with only a 3-Å opening at the cytoplasmic end (determined by examination of the structure from Chang et al., 1998), there must be an enormous change in protein conformation upon channel gating. Here, we have tested the contribution to channel gating of one residue, glycine 22 (G22), which, by analogy to Tb-MscL, would be buried within the wall of the constricted pore (Chang et al., 1998). We have replaced this residue with all 19 other common amino acids and tested the effects on cellular growth and channel gating. Our results suggest a model for the environmental changes that occur in this region of the channel upon transitioning from the closed to the fully-open state.

MATERIALS AND METHODS

Mutagenesis of *mscL*

We have generated all possible 19 amino acid changes at MscL's amino acid 22 using a megaprimer polymerase chain reaction (PCR) strategy (Barik, 1993). This strategy required two rounds of PCR, both using as template the wild-type *mscL* in pB10b (Moe et al., 1998; Ou et al., 1998). The first PCR was primed with either a precise or degenerate oligonucleotide encompassing the codon we wished to change. Synthesis of the complementary strand was primed from 17 nucleotides outside the 3′ end of the open readin frame (ORF) using an Xho1-tagged primer sequence that extended into the pB10b vector: 5′-GTT CGC GGA CTT TCG TCg agc tcg agc tc-3′ (Sukharev et al., 1994). We then used this product as a megaprimer to generate the entire ORF using a BglII-tagged 5′ primer that included the initial ATG (5′-AGA TCT AGA TCT CAT AGG GAG AAT AAC ATG-3′).

The PCR product containing the mutant mscL ORF was then gel purified (QIAGEN Inc., Valencia, CA), digested with XhoI and BglII, and ligated into an antisense plasmid pB10c (Moe et al., 1998). This construct was then transformed by electroporation (Biorad, Hercules, CA) into the *mscL* knockout strain PB104 (Blount et al., 1996c) and the amplified DNA extracted (QIAGEN) for sequencing by the University of Wisconsin Biotechnology Center (Madison, WI), using Amplitaq or BigDye (Perkin-Elmer Biosystems, Foster City, CA). After the engineered amino acid change was detected, the ORF was excised with XhoI and BglII and ligated into the plasmid PB10b, which can express the ORF under the control of a lac-inducible promoter (Moe et al., 1998). All cloning steps and expression were performed within the mscL knockout *E. coli* PB104. Each entire ORF was sequenced through the flanking BglII and XhoI sites described above to ensure that there were no unintended changes.

Bacterial growth assays

Plate assay

Single colony isolates from Luria-Bertani (LB) + amp (ampicillin 100 μg/μL in all cases) (Lech and Brent, 1995) plates of the *mscL*-null *E. coli* PB104 harboring the G22X mutant plasmids were grown overnight in liquid LB + amp. Typically, cells were at an OD_{600} of 1.4 to 1.5 at this point although the slow growing G22D and G22E were at ~1.2. The cells were diluted 1:10 into fresh LB + amp and grown on the shaker at 37°C for an additional hour. Then the cells were serially diluted and plated in the presence or absence of 1 mM isopropyl-β-D-thiogalactoside (IPTG) (Research Products International, Mt. Propsect, IL). The plates were incubated for 19 h at 37°C when growth was scored. The assay was performed at least three times using either one or two single colony isolates during each assay.

Liquid growth

Single colony isolates from LB + amp plates of PB104 harboring the G22X mutant plasmids were grown for 17–18 h in liquid LB + amp at 37°C. Then they were diluted into prewarmed (37°C) medium (100 μL in 2 mL) and grown for an additional 2 h. They were then further diluted to an OD_{650} of 0.02 in 25 mL of prewarmed (37°C) LB + amp, each in a 125-mL flask. The OD_{650} was determined every half hour during the subsequent growth. After 2 h 15 min, IPTG was added to the flask to a final concentration of 1 mM to induce expression of the G22X plasmid. The next OD_{650} reading was taken 20 min later and, thereafter, every 30 min. The growth data from six different experiments using half of the G22X mutants plus controls in each experiment were subjected to statistical analysis and expressed as the mean and the standard deviation of the population (Microsoft Excel, Microsoft Corp., Redmond, WA) at each data point. $n = 3$ or 4 for each G22X mutant and $n = 4$ and $n = 12$ for the knockout strain with the empty vector and wild type, respectively. The growth rate after induction was determined using the LINEST function (Microsoft Excel) on the data generated between time 3:05 h (50 min after induction) and 5:05 h.

Electrophysiological techniques

Spheroplast preparation

E. coli spheroplasts were prepared and wild-type and mutant MscL activity was recorded essentially as previously described (Blount et al., 1999). Cephalexin (final concentration 0.06 mg/mL) was added to log-phase cells growing in modified LB medium that contained 0.5% NaCl instead of 1% NaCl (Martinac et al., 1987). After incubation for 1.5–3 h, IPTG was added (final concentration 1.3 mM) to induce *mscL* expression. The induction time varied from 5 min to 1 h. Longer preincubation and induction were necessary when a mutant with a slow-growth phenotype was used. The cells were then harvested and lysed with lysozyme (0.2 mg/mL), and spheroplasts were collected by centrifugation.

Patch clamping

Electrodes with resistances of 3.5–4.5 MΩ (bubble number = 4.2–4.8) were used to clamp inside-out patches. Pipette solutions contained 200 mM KCl, 90 mM $MgCl_2$, 10 mM $CaCl_2$, and 5 mM Hepes (pH 6.0), whereas the bath solution additionally contained 0.3 M sucrose to stabilize the spheroplasts. Currents were measured with a List EPC 7 amplifier (List Medial, Darmstadt, Germany) and filtered with an 8-pole Bessel filter at 3 kHz. The potential of the pipette was held +20 mV higher than that of the bath. Current recordings were digitized at 10 kHz with Digidata 1200 interface using Clampex ver. 7.0.0.86 software (Axon Inst., Foster City, CA) and stored in a PC. Pressure was applied by syringe-generated suction through the patch-clamp pipette and measured with a pressure guage (143PC05D, Honeywell, Minneapolis, MN).

Data were analyzed using FETCHAN ver. 6.0.5, pSTAT ver. 6.0.5, and AxoGraph ver. 3.5.5 software (Axon Inst.). The kinetics of the channels

that had a high threshold were not examined in all MscL mutants because the pressure needed to activate the MscLs was close to the lysis pressure of the membrane.

Determination of the gating threshold

The threshold of MscL (or mutant MscL) gating was expressed as the ratio of the pressure required to gate MscL (or a mutant MscL channel) relative to that of MscS (Blount et al., 1996a). For mutant MscLs showing an open substate, gating into the substate was defined as the threshold. The absolute value of this threshold varied most likely due to variation in the geometry of the patch (Sukharev et al., 1999b).

RESULTS

The hydrophobicity of amino acid 22 systematically affects the growth of *E. coli* harboring the mutant MscL protein

Plate growth

Bacteria were grown and then plated in serial dilutions on LB + amp plates with or without the inducer, IPTG. When the mutant construct was induced, there was a gradient of growth inhibition that correlated with the hydrophobicity of residue 22 (Fig. 1). In the presence of IPTG, growth was completely absent for bacteria harboring *mscL*s containing the most hydrophilic substitutions at amino acid 22 (Fig. 1 *A*). Substituting an amino acid having an intermediate hydrophobicity, such as proline, tyrosine, or serine, slowed growth. In these cases, growth was evident, but colonies were noticeably smaller after only 19 hr of growth (Fig. 1 *A*) and, after 42 h of growth, colony size was still restricted (data not shown). Hydrophobic substitutions showed no visible effect on growth or viability after 19 h at 37°C (Fig. 1 *A*). Therefore, the hydrophobicity of the substitution at G22 of MscL systematically affected the plate growth of the *mscL*-null strain harboring this construct.

The *mscL* mutants having an acidic residue (aspartate or glutamate) at residue 22 grew poorly even without induction (<1% of wild type, Fig. 1 *A*). The extreme toxicity of the acidic mutations most likely was due to leakage through the *lacUV5* promoter, which allows 0 to 6 units of MscL per patch even without induction (Blount et al., 1997). This extreme growth inhibition in the absence of induction was not seen with basic substitutions at G22, showing that an acidic substitution at residue 22 has an added detrimental effect not yet understood.

Growth in liquid media

The G22X series of strains was also grown in liquid LB + amp as described in Materials and Methods. Cells that were in exponential steady-state growth were induced, and their subsequent growth was followed with optical density measurements at 650 nm. Figure 1 *B* reveals the same three groups highlighted by the growth on plates. Those inhibited by expression of the G22X plasmid, including all basic and some polar substitutions, hug the bottom of the graph. Those significantly slowed by expression of the G22X plasmid, i.e., G22P, G22S, and G22Y, comprise the middle group. Those unaffected by expression of the G22X plasmid, i.e., the remaining hydrophobic substitutions, along with wild type and the knockout plus empty vector, comprise the upper group. The growth rates clearly correlate with the hydrophobicity of the residue 22 substitution (Fig. 1 *C*). Hydrophobicities given here and below are from Kyte and Doolittle (1982). There is a sharp threshold of allowed hydrophobicity at which growth rates vary greatly (for example, 0.37 OD_{650} units/hr for wild type of hydrophobicity −0.40 versus −0.007 OD_{650} units/hr for G22T of hydrophobicity −0.70). On either side of this narrow hydrophobicity threshold between −1.3 and −0.40, growth is either vigorous (up to a hydrophobicity of 4.5) or completely inhibited (down to a hydrophobicity of −4.5) (Fig. 1 *C*).

It was not possible to examine G22D and G22E using the liquid growth assay, because these strains were consistently slow to come out of stationary phase resulting from the overnight growth and were not in steady-state growth at the time of induction.

The threshold for mechanosensitive gating corresponds to the hydrophobicity of residue 22

Channel activity was recorded from excised patches from spheroplasts expressing the various plasmid-borne *mscL* alleles in an *mscL* deletion strain. When negative pressure (suction) was applied to the membrane, two types of channel activities were readily observed. Figure 2 *A*,*ii* shows that MscS (▼), native to all strains, was activated at a lower suction and passed about 25 pA of unitary current (at −20 mV). Wild-type MscL (↕) activated next with greater suction, at a pressure 1.6 times that required to open MscS, and the MscL channel's unitary current was about 80 pA (Fig. 2 *A*,*ii*). Because MscL and MscS gate in response to membrane tension, not pressure, individual patch geometries affect the pressure dependence of activation. To account for variable patch geometries, the gating threshold of MscL (or the mutant G22X channels) is given as the ratio of the suction at which MscL (or the mutant MscL) is found to gate relative to that at which MscS opens (see Materials and Methods). For wild-type MscL, that threshold was 1.64 ± 0.08 (mean ± SD, $n = 9$) over a range of 110–190 mmHg (Table 1).

We determined the gating threshold ratio of each of the G22X MscL channels expressed in an *mscL* knockout background (Table 1). When a hydrophobic residue such as alanine was substituted for glycine 22, higher pressure was required to open this channel (compare G22A and wild type traces, Fig. 2 *A*, *i* and *ii*). The gating threshold pressure ratio of 2.47 ± 0.20 (G22A/MscS, $n = 4$) was significantly higher than the wild-type MscL/MscS ratio (1.64) (Table 1). In contrast, when glycine 22 was substituted with a polar or charged amino acid, the mutant MscL channel was activated

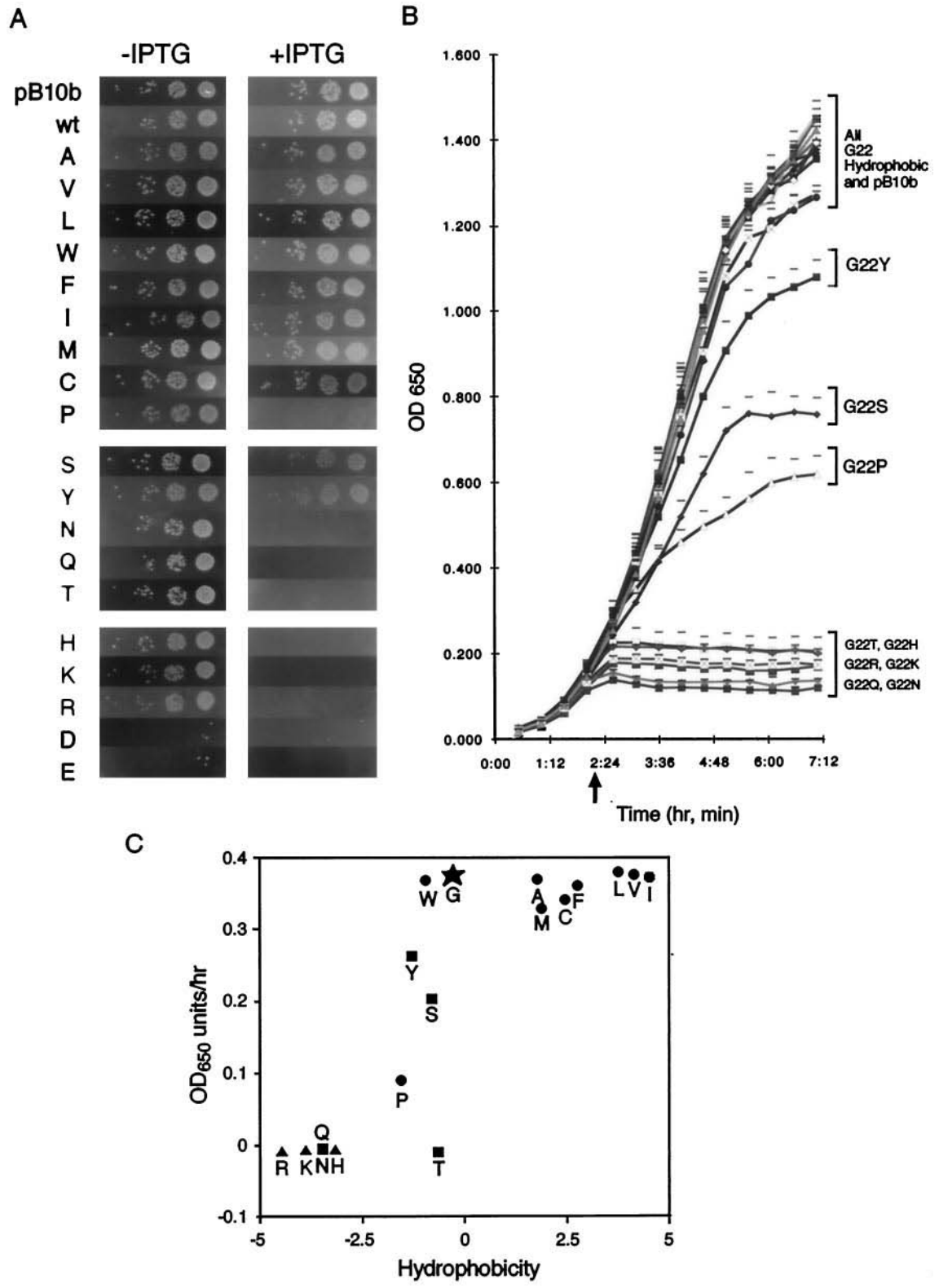

FIGURE 1 (*A*) Growth of *mscL*-null *E. coli* harboring *Lac*-inducible plasmids with G22X inserts. For growth conditions see Materials and Methods. The panels show the growth of 5 μL of each tenfold dilution (10^{-3} to 10^{-6}) of G22X mutants plated in the absence (*left*) or presence (*right*) of IPTG. Each section shows growth of cells containing the following G22X substitutions: hydrophobic (and the empty vector, pB10b), polar, and hydrophilic. (*B*) Summary of the liquid growth of all 20 G22X strains and *mscL*-null cells contaning pB10b. Induction with 1 mM IPTG is indicated by the arrow. Shown are the results of six separate experiments; half of the G22X mutants were tested in each experiment along with wild type and the knockout containing the empty vector. $n = 3$ or 4 for all mutant strains, $n = 12$ for wild type, and $n = 4$ for the knockout with pB10b. The standard deviation of the population is given at each data point. (*C*) Dependence of the liquid culture growth rate on the hydrophobicity of the amino acid at position 22 (Kyte and Doolittle, 1982). The standard code is used to designate the residues at position 22. Amino acid code: glycine (★), hydrophobic (●), polar (■), and basic (▲).

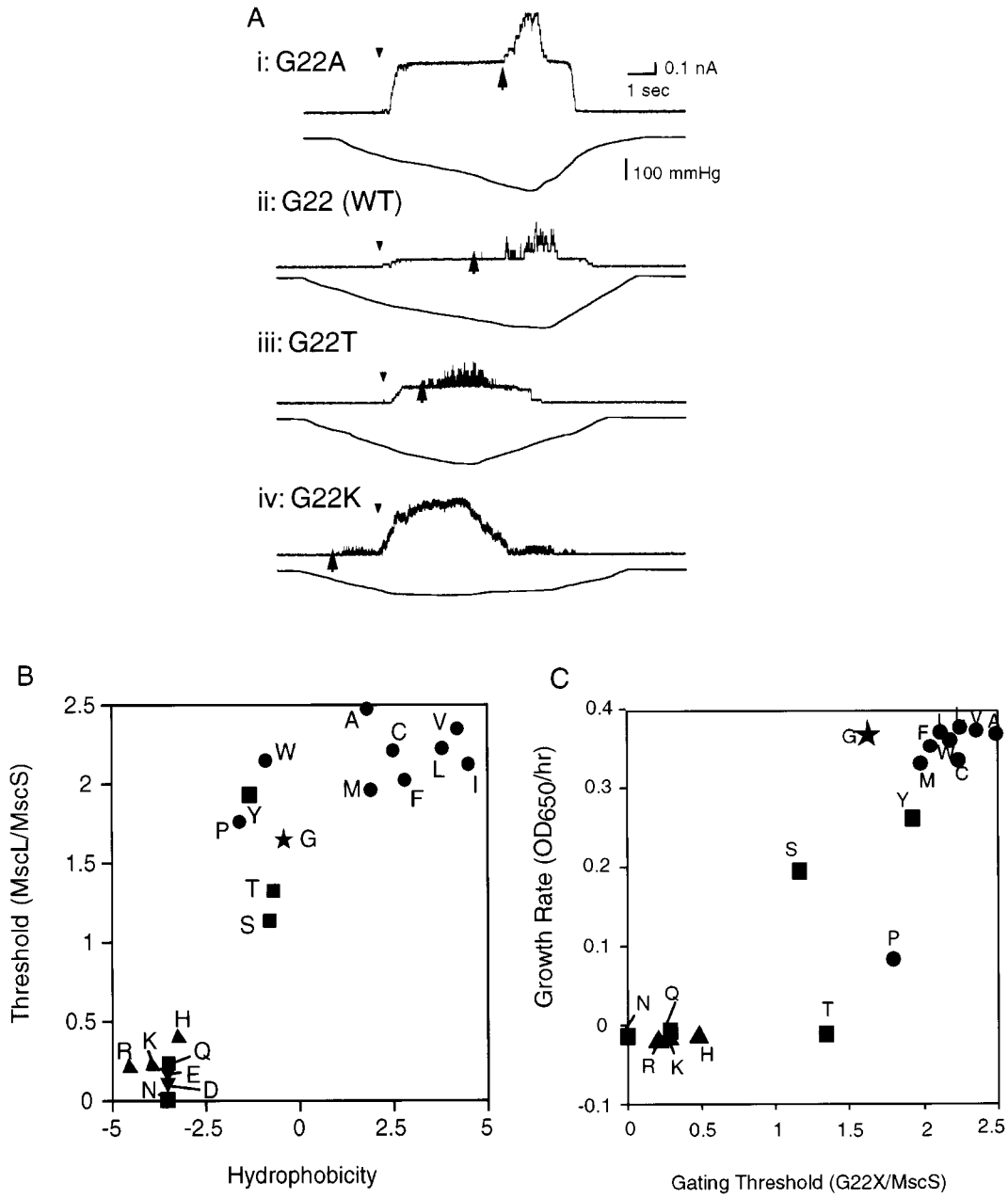

FIGURE 2 (*A*) Channel activity of four G22X MscL substitutions. The traces show the pressure sensitivity of mutant MscL having a specific amino acid at position 22: (*i*) strongly hydrophobic, G22A; (*ii*) wild type, G22; (*iii*) intermediately hydrophilic, G22T; and (*iv*) very hydrophilic, G22K. In each case, the membrane current (*top*) and applied suction (*bottom*) are shown. The first opening of MscS and MscL upon continuously increasing suction is indicated by arrowheads and arrows, respectively. Note the left shift of the arrows as the substitution becomes more hydrophilic from *i* to *iv*. The thresholds for G22A, G22, and G22T are, respectively, 2.54, 1.83, and 1.41 times higher than that for MscS. The threshold for G22K is 0.49 times that of MscS in these traces. (*B*) Dependence of the threshold for activating MscL on the hydrophobicity (Kyte and Doolittle, 1982) of the amino acid at position 22. The threshold of activation of mutant MscL channels is shown as the ratio of their activation pressure to that of MscS. (*C*) G22X gating thresholds versus their growth rates in liquid culture. For (*B*) and (*C*), the letters are standard codes for residue 22. Amino acid code: glycine (★), hydrophobic (●), polar (■), basic (▲), and acidic (▼). Note that ▼ appears in (*B*) only.

at a pressure lower than that required to gate wild-type MscL. For example, the negative pressure required to open the polar substitution mutant G22T was near that required to open MscS, whereas the hydrophilic substitution mutant G22K opened before MscS (Fig. 2 *A*, *iii* and *iv*).

The effect of the hydrophobicity of residue 22 on the gating threshold of all 20 possible G22X substitutions is summarized in Fig. 2 *B* and Table 1. Hydrophilic substitutions eased gating, whereas more hydrophobic substitutions hampered gating. The MscL gating threshold rose from 0 (i.e., the channel was active in the absence of intentionally applied suction) to about 2 in parallel with the increase in hydrophobicity of the amino acid at position 22. The threshold of MscLs with a very hydrophobic substitution may be

TABLE 1 Mechanical sensitivity of the 20 G22X MscLs

MscL	Threshold (relative to MscS)	Hydrophobicity*	MscL	Threshold (relative to MscS)	Hydrophobicity*
G22N	0.00 ± 0.00 (4)	−3.5	G22P	1.76 ± 0.18 (3)	−1.6
G22E	0.10 ± 0.18 (3)	−3.5	G22Y	1.92 ± 0.07 (3)	−1.3
G22D	0.16 ± 0.28 (3)	−3.5	G22M	1.96 ± 0.24 (4)	1.9
G22R	0.21 ± 0.30 (3)	−4.5	G22F	2.02 ± 0.25 (5)	2.8
G22K	0.23 ± 0.27 (3)	−3.9	G22I	2.12 ± 0.04 (3)	4.5
G22Q	0.23 ± 0.21 (3)	−3.5	G22W	2.15 ± 0.33 (3)	−0.9
G22H	0.40 ± 0.26 (3)	−3.2	G22C	2.21 ± 0.23 (3)	2.5
G22S	1.14 ± 0.14 (4)	−0.8	G22L	2.23 ± 0.24 (5)	3.8
G22T	1.32 ± 0.15 (5)	−0.7	G22V	2.35 ± 0.33 (3)	4.2
G22 (WT)	1.64 ± 0.08 (9)	−0.4	G22A	2.47 ± 0.20 (4)	1.8

Data are arranged with MscL threshold value.
*The threshold is shown as the relative value to that of MscS (see Material and Methods). Mean ± standard deviation is shown. Number in parenthesis is the number of spheroplasts examined. Three to five measurements were done on each spheroplast.
**From Kyte and Doolittle (1982).

an underestimate because we sometimes did not observe MscL activity up to the lytic pressure (about 2.5 times the MscS threshold) of the patch membrane. The sign of the charge that leads to hydrophilicity did not affect the threshold at our resolution (compare G22R or G22K with G22D or G22E, Fig. 2 *B* and Table 1).

Combining the results presented in Fig. 2, *A* and *B*, one can see that the growth rates of the G22X mutants largely correlate with the gating thresholds of their MscL channels (Fig. 2 *C*). Although the relationship is clear for cells harboring channels whose residue 22 is clearly more or less hydrophobic than glycine, the relationship breaks down for G22X mutants for which the hydrophobicity of residue 22 is close to that of glycine.

The hydrophobicity of amino acid 22 affects dwell times in the fully open state and in an open substate

The wild-type MscL channel gates through several transient subconductance states to the fully open state of about 3 nS upon the application of a membrane tension (Fig. 3 *A*,*ii* and Sukharev et al., 1994). Its full-open time distribution (Fig. 3 *B*,*ii*) can be fitted with three Gaussian components dominated by the one with a time constant of about 20 ms. In this study, we registered the three time constants (T) and their proportions (in parentheses) to be 19.4 ± 2.5 ms (0.67), 2.5 ± 1.1 ms (0.09), and 0.1 ± 0.1 ms (0.24, $n = 3$), not significantly different from those previously reported (Fig. 3 *B*,*ii* and Blount et al., 1996b).

Replacing G22 with the more hydrophobic alanine caused a large increase in open dwell. Here, the open time was largely accounted for by a single Gaussian distribution with a T of 145 ± 33 ms (Fig. 3 *B*,*i*). Continuous openings for over 0.5 s were often encountered (Fig. 3 *B*,*i*). Substitutions with other hydrophobic residues gave openings similar to wild type (Fig. 3 *C*).

In contrast, replacing G22 with threonine, a mildly hydrophilic residue, shortened the open dwell, now dominated by events at or below 2 ms (T = 0.91 ± 0.28 ms) (Fig. 3 *B*,*iii*). This gave the flickery impression of the mutant channel activities (Fig. 3 *A*,*iii*). Substitutions with two other mildly hydrophobic residues, P and S, gave results more similar to wild type (Fig. 3 *C*).

Replacing G22 with a charged or strongly polar residue yielded channel activities that were very flickery, e.g., G22K MscL activity had a fully open dwell dominated by events shorter than 0.5 ms (T = 0.24 ± 0.08 ms, Fig. 3 *A*,*iv* and *B*,*iv*). In addition, these channels also lingered in a subconductance state. Fig. 3 *A*,*iv* and its inset show dwells in such a substate for tens of milliseconds (T = 11.0 and 1.1 ms) in the case of G22K. Here the substate conductance is about 0.5 nS in conductance, about ⅕ of the full unitary conductance, and most similar to the conductance of the lowest substate in the wild type (Sukharev et al., 1999b). Wild-type MscL rarely stays in this subconductance state for more than 1 ms. Substitution of G22 with the positively charged R, K, or H, the negatively charged D, or their amine equivalents, N or Q, all resulted in this cluster of biophysical phenotypes: low gating threshold, flickery activity, and a stable substate at or near the lowest subconductance level (Fig. 3 *C*). G22E showed a stable substate but had a channel opening (9.9 ms) longer than these mutant MscLs. The results indicate that these toxic channels (Fig. 1) disfavor the closed states, but, among the open states, they favor the lowest subconductance state over the fully-open state at intermediate open probability.

Hypersensitive mutant MscLs are pressure sensitive at all states

When an increasing suction ramp was applied to the membrane containing hypersensitive mutant MscL channels, the prominent lowest open substate appeared first and the full-open state occurred at higher pressure. Thus, such mutant MscLs first go through a low-threshold C-to-S transition and then, with increasing pressure, through a high-threshold S-to-O transition, where C is the closed, S is the first

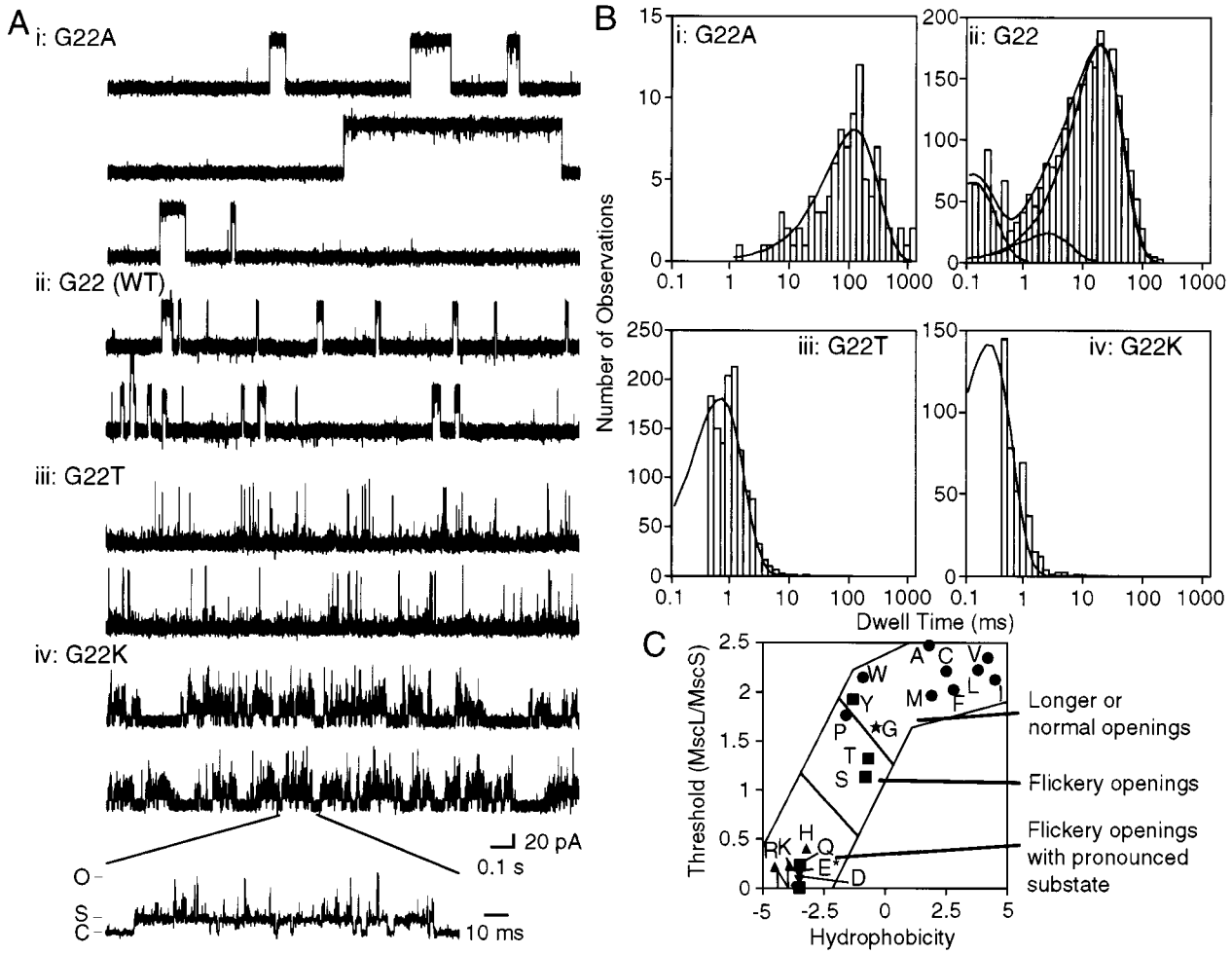

FIGURE 3 (*A*) Single channel openings and (*B*) dwell time histogram of (*i*) G22A, (*ii*) wild type MscL, (*iii*) G22T, and (*iv*) G22K. (*C*) Classification of channel kinetics of wild type and G22 substituted MscLs. The channel kinetics are grouped into three classes according to the mean channel open time (flickery: $\tau < 2$ ms versus normal or long: $\tau > 10$ ms; the longest time constant is used if there were more than two components) and the presence of an open substate. The channel open time of G22E (*) was 9.9 ms, which is not flickery by this definition. The letters are standard codes for residue 22. Amino acid code: glycine (★), hydrophobic (●), polar (■), basic (▲), and acidic (▼).

substate, and O is the fully-open state. We tested the mechanosensitivity of different states by evaluating the transitions at different pressures for G22N MscL, a channel that is active even in the absence of applied suction (Fig. 4).

Without suction, G22N fluctuated mainly between the closed and the open substate without full opening (Fig. 4 *A*, *top trace*). When a moderate suction was applied to the membrane (105 mmHg), the channel largely remained in the substate but flickered to the fully open state (Fig. 4 *A*, *middle trace*). The closed state was infrequent, indicating that the C-to-S transition was almost saturated toward S. When a higher pressure was applied (210 mmHg), the channel stayed mostly in the fully-open state and flickered back to the substate, as its S-to-O transition approached saturation (Fig. 4 *A*, *bottom trace*). These recordings at static pressures confirmed the observation in the pressure-ramp experiment. We next used such data for the quantitative evaluation of the mechanosensitivity of each transition.

If we assume a serial three-state model, in which the channel is in one of the three states, C, S, or O, the equilibrium can be expressed as

$$C \leftrightarrow S \leftrightarrow O. \tag{1}$$

If we express the probability of being in the closed, substate, and fully-open state as P_C, P_S, and P_O, respectively (thus $P_C + P_S + P_O = 1$); the probability of the channel being on the right side of the C-to-S transition is

$$P_{CS} = P_S + P_O, \tag{2}$$

where P_S and P_O are the probability of being in the substate and in the fully open state, respectively. Similarly, the probability of the open channel being on the right side of the S-to-O transition is

$$P_{SO} = P_O/(P_O + P_S). \tag{3}$$

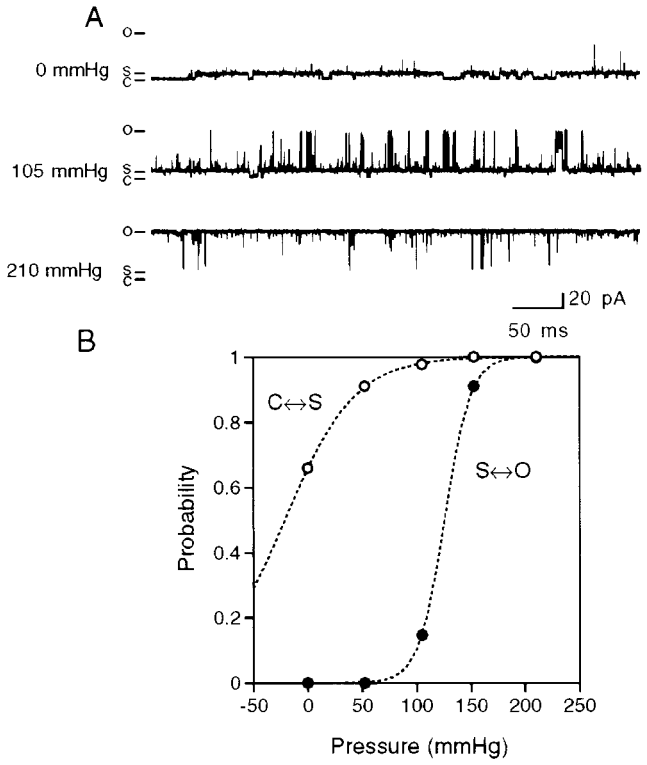

FIGURE 4 Pressure dependence of the transition from closed state to substate and from substate to fully open state in a hypersensitive mutant MscL, G22N. (*A*) Current trace. O, S, and C indicate the open, sub-, and closed states, respectively. (*B*) Probability of the transition from closed to substate (*open symbol*) and from substate to fully-open state (*closed symbol*). Lines indicate the Boltzman curves fitted to the experimental data. The threshold of MscS in this patch was 145 mmHg. Therefore, the threshold for the wild-type MscL would be about 240 mmHg because the wild-type threshold ratio (MscL/MscS) is 1.64.

These probabilities are equivalent to the channel open probability used in usual kinetic studies. We found that P_{CS} and P_{SO} both increase with pressure but clearly in a different pressure range (Fig. 4 *B*). The C-to-S transition occurs at much lower pressure than the S-to-O transition. Each component was fit to a Boltzmann's curve,

$$P = \frac{\exp[(p - p_{1/2})/s_p]}{1 + \exp[(p - p_{1/2})/s_p]} \quad (4)$$

where $p_{1/2}$ is the pressure required to attain half-maximal probability, and s_p is the slope of the plot of $\ln[P/(1 - P)]$ versus pressure (Martinac et al., 1987). The $p_{1/2}$ was 56 ± 37 mmHg for the C-to-S transition and 132 ± 18 mmHg for the S-to-O transition ($n = 3$). This indicates that the fully open state is brought about by at least two steps that are distinct with respect to conductance and pressure sensitivity. All mutant MscLs of the lower group in Fig. 3 *C* behaved in a manner similar to G22N. Quantitative analysis on another member of this group, G22D, gave results similar to those of G22N shown here.

pH Affects the mechanosensitivity of G22H MscL

Because the hydrophobicity of residue 22 governs mechanical gating and channel kinetics, one might expect that these parameters would change with pH, if H^+ is accessible to histidine 22 of G22H MscL. Because histidine has a pK_a of 6.5, we examined the activities of G22H MscL at pH 6.0 and at pH 7.5. Preliminary experiments at a lower pH (pH 5.0) in the bath and/or pipette solution showed little difference from results obtained at pH 6.

When the pH of the bath solution (i.e., the cytoplasmic side of an inside-out patch) was 6.0, which allows the histidine (if exposed) to become more positively charged from the cytoplasmic side of the channel, the G22H channel acted like a hydrophilic substitution mutant. It opened with very little suction: it gated at a suction that was less than half that required to open MscS (Fig. 5 *A*, *left side*). With increasing suction, G22H showed two conductance states: an open substate with an amplitude of about 20 pA and a full-open state with an amplitude of about 80 pA (all at −20 mV). When the pH of the bath solution was increased from pH 6.0 to 7.5 by perfusion, the G22H channel acted like a channel with an uncharged residue 22, and opening G22H required greater suction than that required to gate MscS (Fig. 5 *A*, *right side*. Note the reordering of the two thresholds marked by the arrow for G22H and MscL, and the arrowhead for MscS). This change was reversible. A paired *t*-test of the change in the pressure needed to activate G22H MscL (48 ± 10 mmHg at pH 6.0 and 156 ± 63 mmHg at pH 7.5, $p < 0.05$, $n = 3$) indicated a significant decrease in sensitivity with this increase in pH on the cytoplasmic side. In contrast, the sensitivity of wild-type MscL was not affected by the pH of the bath solution (Fig. 5 *B* and Blount et al., 1996c).

These results showed that histidine 22 was accessible to cytoplasmic H^+. To examine the effect of periplasmic pH, the tip of the pipette was filled with pH 6.0 solution (with 0.3 M sucrose, to prevent immediate mixing) and backfilled with pH 7.5 solution (without sucrose, to allow a gradual change in pH at the extracellular side) (Blount et al., 1996c). The suction needed to gate G22H MscL was half that needed to open MscS within 10 min after filling the pipette and before significant mixing of the pH 6.0 and pH 7.5 solutions (Fig. 5 *C*, *left side*). When the same patch was examined after 1 h, the G22H MscL opened only when a suction greater than that needed to open MscS was applied (Fig. 5 *C*, *right side*). A paired *t*-test (52 ± 13 mmHg at pH 6.0 and 152 ± 57 mmHg at pH 7.5, $p < 0.05$, $n = 3$) indicated that this increase was also statistically significant. In the converse experiment of tip filling at pH 7.5 and back filling at pH 6.0, we observed the reverse change, i.e., the G22H channel first had a high and then a low pressure threshold (data not shown). The sensitivity of wild-type MscL did not change with the periplasmic pH (Fig. 5 *D*). The change in the gating threshold of G22H MscL was not simply dependent on time because the sensitivity did not change when the pipette and bath solution were both kept at

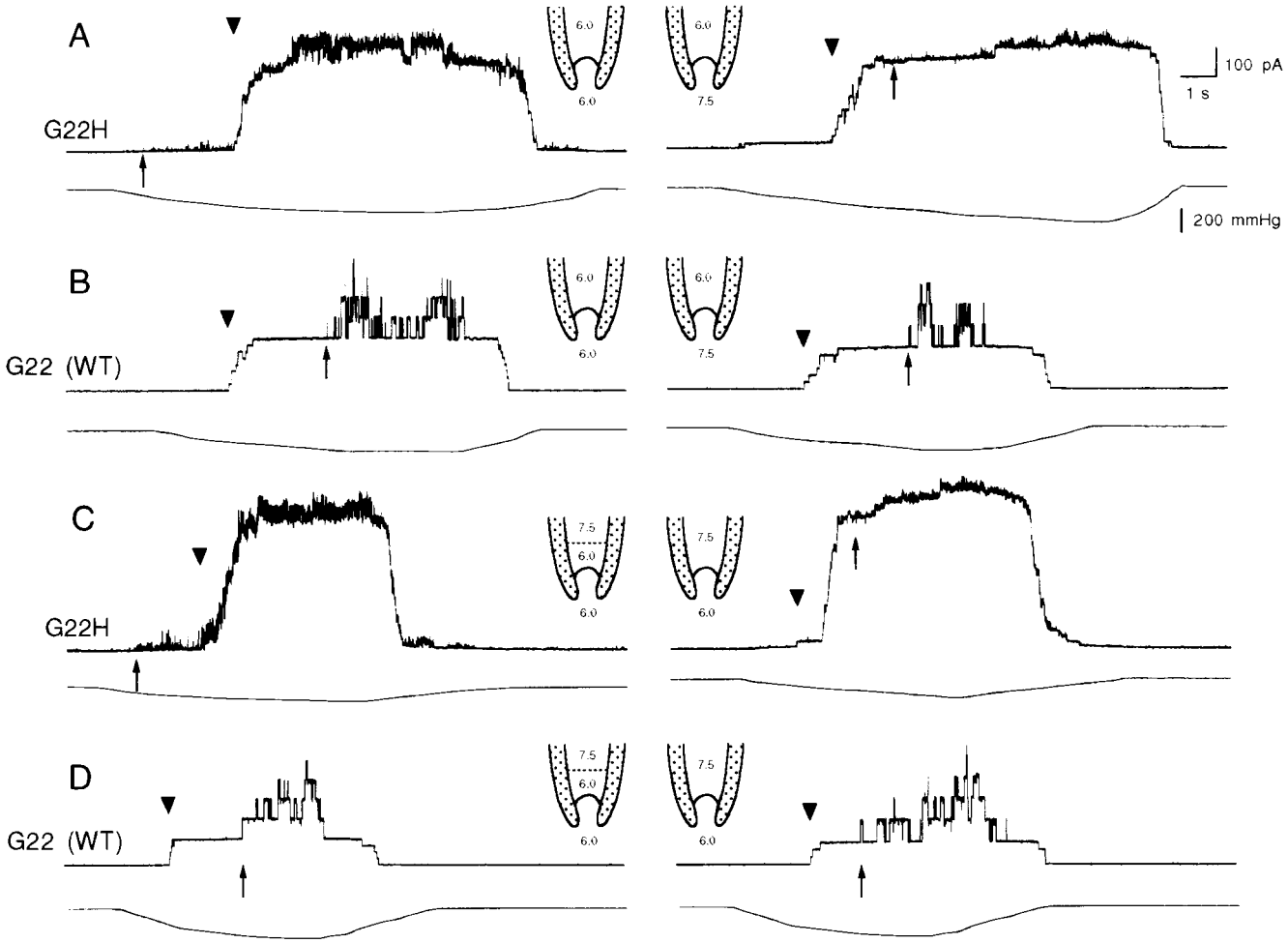

FIGURE 5 Change of mechanosensitivity of (*A*, *C*) G22H and (*B*, *D*) wild-type MscL with pH using the inside-out patch configuration. (*A*, *B*) pH of the cytoplasmic side was increased by changing the pH of the bath solution. The pH of the bath solution was 6.0 (*left trace*) and 7.5 (*right trace*). (*C*, *D*) The pH of the periplasmic side was changed by filling the tip of the pipette with pH 6.0 solution and back-filling it with pH 7.5 solution. The channel activities examined within 10 min (*left trace*) and 1 h after back filling (*right trace*) are shown. The inset shows the pH of the pipette and bath solution.

pH 6.0 for up to two hours (data not shown). When both the pipette and bath were at pH 7.5, the threshold also did not change with time; again, more suction was required to gate G22H than MscS as in the pH 6.0/pH 7.5 experiments shown above (data not shown). These data suggest that 22H is accessible to protons from both sides of the membrane.

DISCUSSION

Besides being the smallest amino acid, glycine is a residue of intermediate hydrophobicity (Kyte and Doolittle, 1982 and Table 1). G22 is located in the first transmembrane helix of MscL and is largely conserved, although alanine is an allowed substitute in more distant bacterial homologues (Sukharev et al., 1997; Chang et al., 1998; Moe et al., 1998). By analogy with the *M. tuberculosis*-MscL structure, this glycine is virtually buried just under the outermost constriction of the closed channel and faces an adjacent subunit helix, which also contributes to the closed pore (Chang et al., 1998, Batiza et al., 1999). Changing glycine 22 of *E. coli*'s MscL to a more hydrophobic residue (Table 1) results in a channel that requires greater tension to open (Fig. 2) and that has a comparable (or longer) dwell time in the fully open state (Fig. 3). However, the bacteria tolerate these changes well (Fig. 1). In contrast, hydrophilic substitutions at G22 reduce cell viability (Fig. 1). They result in easy gating of the mutant mscL channel (Fig. 2) and channel flickering in the fully open state (Fig. 3) with the exception of G22E (see Results). The most hydrophilic substitutions also reveal the presence of a stable open substate (Figs. 3 and 4). No other parameter of the side chains, such as the sign of charge and the size of side chain, seems to correlate with the gating defects systematically. For example, the G22A and G22I substitutions have almost identical effects on channel kinetics (Fig. 3) and cell growth (Fig. 1) although the size differs significantly (the van der Waals volumes of alanine and isoleucine are 67 Å and 124 Å, respectively).

Our data indicate the relative hydrophobicity of a residue's environment inside the gate before, during, and pos-

sibly after opening (Fig. 6 *A*). A change to a more hydrophobic amino acid at residue 22 makes the channel harder to open, whereas a more hydrophilic amino acid at residue 22 makes the channel open more easily to a substate (Fig. 2). Thus, the hydrophobicity of residue 22 affects the energy barrier between the closed state and the first open substate. [Note that the transition between the closed state and the first open substate is the major pressure-dependent step in wild-type gating (Sukharev et al., 1999b)]. More hydrophobic substitutions increase this barrier, whereas more hydrophilic substitutions decrease this barrier. Every logical explanation that accounts for these specific changes (i.e., changing the depths of the energy wells and/or the height of the transition barrier peak) requires residue 22 to be in a relatively more hydrophobic environment in the closed state than in the open substate (Fig. 6 *A*, closed state and open substate).

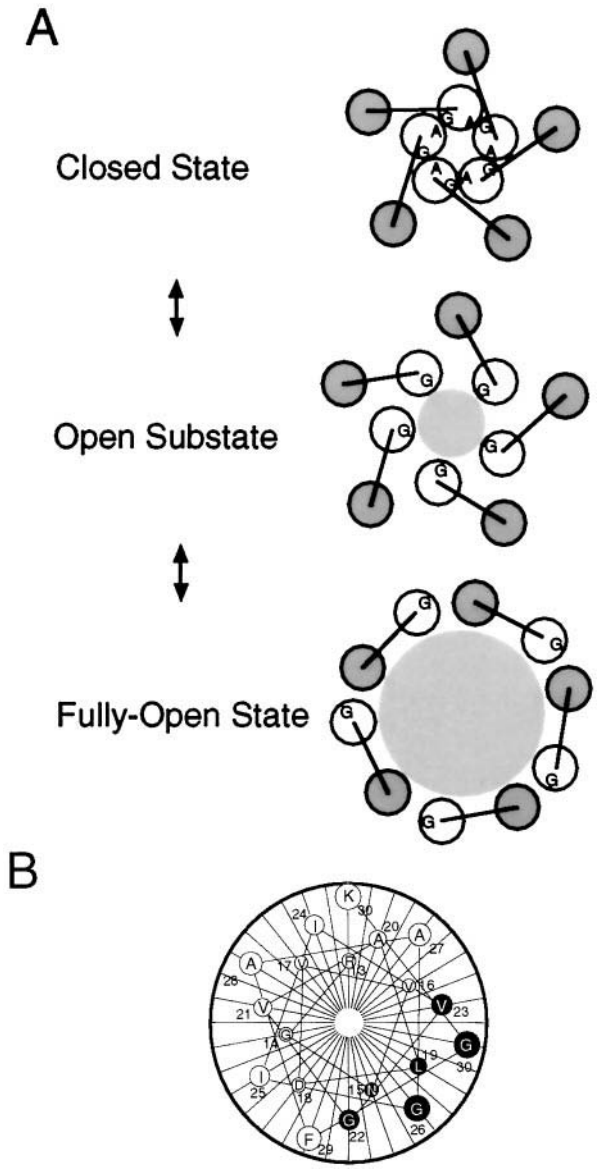

FIGURE 6 (*A*) Model for the position of G22 during channel opening. Transverse section of M1 (*open circle*) and M2 (*shaded circle*) at the level of G22 viewed from the periplasmic side. M1 and M2 of each subunit are connected with a line. Residues G22 (*G*) and A20 (*A*) are highlighted on each M1 helix of MscL. The shaded area at the center indicates the lumen filled with water. (*B*) Mutants in M1 of MscL highlighted (in *black*) in the GOF screen by Ou et al. (1998). The diagram shows the partial helical wheel of residues 13–30.

The dwell-time kinetics (Fig. 3) may reveal more details about the environment of residue 22. Based upon the closing rate constant data presented by Sukharev and coworkers, WT exhibits a 9-fold increase in the open dwell-time over the pressure range of opening MscL in reconstituted liposomes (Sukharev et al., 1999b). Because the dwell time determinations for the G22X mutants were made at $P_O < 0.1$ (Fig. 3 *B*), by necessity, the pressures at which these measurements were made varied considerably depending upon the particular G22X gating threshold. In addition, the measurements presented here were made of channels in spheroplasts. Given these caveats, the trends presented here suggest that the hydrophilicity of this substitution decreases the open dwell time about 2–3 fold greater than that expected in wild type. Thus, the rates of the backward reactions (O→S) increase with the hydrophilicity of the G22X substitution; therefore, the hydrophilicity of residue 22 decreases the energy barrier between the fully open state and the open substate, suggesting that residue 22 is in a more hydrophobic environment in the fully open state than it is in the open substate (Fig. 6 *A*, open substate and fully open state).

Given the strong sequence conservation, the closed conformation of the *M. tuberculosis* homologue (Chang et al., 1998) presumably describes that of the *E. coli* MscL channel as well (Batiza et al., 1999). The crystallographic structure of Tb-MscL shows that, in the closed state, residues I14 through V21 define the closed gate presumably restricting water passage within. The corresponding residues in *E. coli* MscL are V16 through V23. Tb-MscL's A20 (which corresponds to *E. coli*'s G22) is buried within the walls of this closed fist, because it is in van der Waals contact with Tb-A18 (which corresponds to A20 in *E. coli*) in an adjacent TM1 helix. Therefore, *E. coli*'s G22 would likely be within a hydrophobic environment in the closed state (Fig. 6 *A*, closed). This is consistent with our conclusion that G22 is in a more hydrophobic environment when the channel is closed than when it is partially open.

One would expect large movements of the transmembrane helices during opening to account for the increase from 0 to 3 nS in conductance. M1, in particular, is expected to swing toward the periphery, to straighten up, and, perhaps, to rotate around its own long axis in the process (Chang et al., 1998). The cytoplasmic end of M1 is expected to traverse a distance of some 15 Å, because sieving (Cruickshank et al., 1997) and conductance analyses (Cruickshank et al., 1997; Sukharev et al., 1999b) estimate the fully-open pore to be 30–40 Å in diameter. This requires all transmembrane helices to line the fully open pore (Cruickshank et al., 1997; Chang et al., 1998; Sukharev et al., 1999b). Our data suggest that, during this movement,

residue 22 is in a hydrophilic environment (possibly facing the aqueous lumen) in a partially open state that corresponds to the subconductance state favored when the residue is charged (Fig. 6 *A*, open substate). In the fully open state at the end of this movement, our dwell-time data are best explained by placing residue 22 in a more hydrophobic environment relative to the open substate, such as its being in contact with hydrophobic residues of a neighboring M2 (Fig. 6 *A*, fully open state) or possibly in contact with the lipid bilayer. To achieve this, M1 may rotate clockwise or counterclockwise (Fig. 6 *A*, fully open state) to minimize previously buried hydrophobic surfaces now exposed to the lumen (Chang et al., 1998; Batiza et al., 1999). However, one cannot rule out residue 22's being exposed to the lumen in the fully open state.

G26 and L19, among other M1 residues including G22, were also highlighted by the GOF screen by Ou and colleagues after random mutagenesis (Ou et al., 1998) (Fig. 6 *B*). By analogy with the Tb-MscL structure, L19, G22, and G26 would be near corresponding residues V17, A20, and I24 in an adjacent M1 domain when the channel is closed (Chang et al., 1998, 1msl). The recovered mutants of G26S, L19Y, and G22D, N, and S, were all changes to more hydrophilic residues, and these mutations all resulted in "severe" or "very severe" growth defects, an increase in the sensitivity to stretch, and flickering kinetics (Ou et al., 1998). These results corroborate the present interpretation of the G22 results: a hydrophilic substitution at these residues disrupts the hydrophobic interactions that keep the channel closed. The model for MscL opening defined by our results (Fig. 6 *A*) suggests that this face of M1 highlighted by the Ou et al. (1998) GOF mutants (Fig. 6 *B*) might experience environmental changes during channel opening similar to those proposed for G22. These results also underscore the rationale for conservation of glycine, a residue of intermediate hydrophobicity, at amino acid 22. Glycine 22 is presumably one of several residues defining the constricted region of the pore that oppose the tension required for gating. Any deviation changes the gating properties of the MscL channel. Five MscL homologues having a glycine at this position that were tested by Moe and coworkers opened at a tension similar to that required to open wild type (Moe et al., 1998). However, the MscL homologues of *Staphylococcus aureus*, *Synechocystis*, and *M. tuberculosis* have an alanine at this relative position. Although *S. aureus* opens at a tension similar to that of wild type, *Synechocystis* requires three times the suction of MscS to open (Moe et al., 1998), a value similar to the 2.47 gating threshold ratio of G22A (Table 1). It will be interesting to see whether or not the Tb-MscL channel is relatively stiff.

Interestingly, none of the residues in an adjacent M1 helix presumably close to L19, G22, and G26 in the closed channel (i.e., V17, A20, or I24 on the opposite face of the M1 helix) was recovered in the Ou and coworkers' screen (1998). This suggests that V17, A20, and I24 do not undergo environmental changes similar to those of L19, G22, and G26. They may remain in a hydrophobic environment throughout the gating process, shielded by the adjacent helices and the lipid bilayer.

Arkin et al. (1998) have shown by amide H^+/D^+ exchange that two-thirds of the whole MscL protein is water accessible and suggested that MscL may have a wide aqueous vestibule. However, the length of the closed gate revealed by the Tb-MscL structure (Chang et al., 1998) makes it surprising that the G22H MscL changed its sensitivity when either the bath or pipette solution was changed to pH 7.5 (Fig. 5). This was not due to proton leakage because 1) the high pH (i.e., low proton concentration) determines the sensitivity, 2) the seal resistance is as high as about 4 GΩ, and 3) this occurs even when the pH of the pipette (held +20 mV relative to potential in the bath) was higher than that of the bath. Therefore, this histidine is accessible to protons from either the top or bottom of the channel. The accessibility from both sides may be due to the presence of two protonation sites in histidine and a cleft induced by the increased size of residue 22, and/or multiple conformations in the closed state.

The increase in open probability of MscL with membrane tension has been attributed largely to a decrease in channel closed time. Sukharev et al. (1999b) examined the tension dependence of the transitions among the closed state, several open substates, and the fully open state in wild-type MscL. They identified at least three substates in the wild-type MscL, which occur much less frequently than the substate revealed by the present G22X MscLs. Only one of the transitions, namely from the closed to the first substate ($C \leftrightarrow S_1$), was shown to be dramatically tension dependent. Their results can also be interpreted to mean that other transitions occur at tensions lower than that for the $C \leftrightarrow S_1$ transition in the wild-type. We used the opportunity presented by the G22N MscL with its prominent S_1 and found both $C \leftrightarrow S$ and $S \leftrightarrow O$ to be mechanosensitive. We found that the tension needed for the S-to-O transition (100–150 mmHg) is lower than the suction required for the C-to-S transition (160–300 mmHg). Thus, in the G22N MscL, and probably in wild-type MscL as well, membrane tension pulls on M1 through all stages of gating.

An electromechanical model by Gu et al. (1998) indicates that a domain of the N-terminus region of MscL swings as a gate. The gating is proposed to be brought about by tilting the coulombic forces between the charged residues of the N-terminal, C-terminal, and membrane spanning domains. Our finding that the sign of the charge at position 22 is not important in determining the tension sensitivity is not consistent with this model. We suspect that the hydrophobic interaction, rather than electrostatic interaction, will play a significant role in gating because the latter force is relatively low across the aqueous phase of the lumen.

We are pleasantly surprised by the way in which the hydrophobicity of residue 22 can predict both a biophysical parameter, the gating threshold (Fig. 2), and a complex physiological one, the growth rate (Fig. 1). Figure 2 *C* shows that the gating threshold correlates well with the growth rate. However, the parallel is not complete. Several

factors may contribute to inconsistencies for channels having a substituted amino acid whose hydrophobicity is close to that of glycine. Perhaps some parameter for which glycine has been precisely chosen, in addition to its effect on the gating threshold, contributes to MscL functioning during cell growth. Also, variation in the amount of channel protein expressed in each type of transformant is possible, and the growth rates may be affected by these differences. Nonetheless, the correlation between the mutant MscL's gating behavior and the growth rate of the mutant population seems remarkable, given that one describes a physical parameter of a single protein in vitro, whereas the other describes a characteristic of a population of living cells. Additionally, most of the growth-sensitive channels described here are more sensitive to stretch, but not all have flickery openings (Figs. 1 and 3), suggesting that the former but not necessarily the latter is detrimental to growth. Both of the mutants having acidic substitutions are unusually poor growers, perhaps due to charge-specific filtering when the channel is in the partially-open substate.

Plants, fungi, bacteria, and other walled cells maintain a large turgor that is used to disrupt the bonds cementing wall material so that new wall can be added during growth (Koch and Woeste, 1992). MscLs that activate at lower tensions interfere with growth, presumably because the turgor needed for growth cannot be attained due to channel opening (Fig. 2 *C*). MscLs with a threshold higher than normal do not affect growth possibly because the cells can maintain normal turgor, and MscL is not activated at normal membrane tension. In contrast, the huge turgor imposed by a severe hypo-osmotic shock requires pressure valves to jettison solutes from the swollen cell. Although it has been postulated that mechanosensitive channels serve this function (Berrier et al., 1992; Ajouz et al., 1998), two recent reports substantiate this idea: 1) Heterologously expressing MscL rescues the marine bacterium *Vibrio alginolyticus* from lysis upon osmotic downshock (Nakamaru et al., 1999); and 2) although YggB is necessary for MscS activity, the double mutant *mscL*$^{-}$*yggB*$^{-}$ lyses after a severe hypotonic shock (Levina et al., 1999). It would be interesting to find out which of the G22X channels can protect these organisms from downshock lysis.

In summary, the intermediate hydrophobicity of G22 is a key element of MscL channel's pressure sensitivity and possibly, the dwell time. When this residue is altered, the hydrophobicity of the substitution determines the channel gating characteristics and cell viability. In addition, changing G22 to a hydrophilic residue reveals a pressure-dependent open substate, and further analysis shows that both this substate and the fully open state are pressure sensitive in hypersensitive mutants. A model for moving G22 into different environments during gating has been proposed, which is consistent with the recently published structure of Tb-MscL (Chang et al., 1998). This comprehensive analysis can be applied to other highly conserved channel residues to further dissect mechanosensitive gating.

The authors thank Yoshiro Saimi and Steve Loukin for many helpful discussions regarding the conclusions of this study. We also are indebted to Jean Yves Sgro of the Institute for Molecular Biology and Doug Davies of the Enzyme Institute, both at the University of Wisconsin, Madison, for assistance in analyzing the Tb-MscL structure. We also thank Leanne Olds for assistance in preparing figures. This study was supported by National Institutes of Health grant GM 47856 and the visit of K.Y. was supported by the Ministry of Education, Science, Sport, and Culture of Japan.

REFERENCES

Arkin, I. T., S. I. Sukharev, P. Blount, C. Kung, and A. T. Brünger. 1998. Helicity, membrane incorporation, orientation and thermal stability of the large conductance mechanosensitve ion channel from *E. coli. Biochim. Biophys. Acta.* 1369:131–140.

Ajouz, B., C. Berrier, A. Garrigues, M. Besnard, and A. Ghazi. 1998. Release of thioredoxin via the mechanosensitive channel MscL during osmotic downshock of *Escherichia coli* cells. *J. Biol. Chem.* 273: 26670–26674.

Bargmann, C. 1994. Molecular mechanisms of mechanosensation? *Cell.* 78:729–731.

Barik, S. 1993. Site-directed mutagenesis by double polymerase chain reaction: megaprimer method. *In* PCR Protocols, Current Methods and Applications. Humana Press, Totowa, NJ. 277–286.

Batiza, A., I. Rayment, and C. Kung. 1999. Channel gate! Tension, leak and disclosure. *Structure.* 7:R99–R103.

Berrier, C., A. Coulombe, C. Houssin, and A. Ghazi. 1989. A patch-clamp study of ion channels of inner and outer membranes and of contact zones of *E. coli* fused into giant liposomes. Pressure-activated channels are located in the inner membrane. *FEBS Lett.* 259:27–32.

Berrier, C., C. Coulombe, I. Szabó, M. Zoratti, and A. Ghazi. 1992. Gadoliniumion inhibits loss of metabolites induced by osmotic downshock, and large-stretch-activated channels in bacteria. *Eur. J. Biochem.* 206:559–565.

Berrier, C., M. Besnard, B. Ajouz, A. Coulombe, and A. Ghazi. 1996. Multiple mechanosensitive ion channels from *Escherichia coli*, activated at different thresholds of applied pressure. *J. Memb. Biol.* 151:175–187.

Blount, P., S. I. Sukharev, P. C. Moe, S. K. Nagle, and C. Kung. 1996a. Towards an understanding of the structural and functional properties of MscL, a mechanosensitive channel in bacteria. *Biol. Cell.* 87:1–8.

Blount, P., S. I. Sukharev, M. J. Schroeder, S. K. Nagle, and C. Kung. 1996b. Single residue substitutions that change the gating properties of a mechanosensitive channel in *Escherichia coli. Proc. Nat. Acad. Sci. USA.* 93:11652–11657.

Blount, P., S. I. Sukharev, P. C. Moe, M. J. Schroeder, H. R. Guy, and C. Kung. 1996c. Membrane topology and multimeric structure of a mechanosensitive channel protein of *Escherichia coli. EMBO J.* 15: 4798–4805.

Blount, P., M. J. Schroeder, and C. Kung. 1997. Mutations in a bacterial mechanosensitive channel change the cellular response to osmotic stress. *J. Biol. Chem.* 272:32150–32157.

Blount P., S. Sukharev, P. Moe, B. Martinac, and C. Kung. 1999. Mechanosensitive channels of bacteria. *In* Methods in Enzymology, P. M. Conn editor. Academic Press, San Diego, CA. 458–482.

Chang, G., R. H. Spencer, A. T. Lee, M. T. Barclay, and D. C. Rees. 1998. Structure of the MscL homolog from *Mycobacterium tuberculosis*: a gated mechanosensitive ion channel. *Science.* 282:2220–2226.

Christensen, O. 1987. Mediation of cell volume regulation by Ca influx through stretch-activated channels. *Nature*. 330:66–68.

Cruickshank, C. C., R. F. Minchin, A. C. Ledain, and B. Martinac. 1997. Estimation of the pore size of the large-conductance mechanosensitive ion channel of *Escherichia coli. Biophys. J.* 73:1925–1931.

French, A. S. 1992. Mechanotransduction. *Annu. Rev. Physiol.* 54: 135–152.

Gu, L., W. Liu, and B. Martinac. 1998. Electrochemical coupling model of gating the large mechanosensitive ion channel (MscL) of *Escherichia coli* by mechanical force. *Biophys. J.* 74:2889–2902.

Hamill, O. P., and D. W. McBride, Jr. 1996. The pharmacology of mechanogated membrane ion channels. *Pharmacol. Rev.* 48:231–252.

Häse, C. C., R. F. Minchin, A. Kloda, and B. Martinac. 1997. Cross-linking studies and membrane localization and assembly of radiolabelled large mechanosensitive ion channel (MscL) of *Escherichia coli. Biochem. Biophys. Res. Comm.* 232:777–782

Kernan, M. 1997. The molecular basis of the mechanical senses: one mechanism or many? *J. NIH Res.* 9:32–36.

Koch, A. L., and S. Woeste. 1992. Elasticity of the sacculus of *Escherichia coli. J. Bacteriol.* 174:4811–4819.

Kyte, J., and R. F. Doolittle. 1982. A simple method for displaying the hydropathic character of a protein. *J. Mol. Biol.* 157:105–132.

Lansman, J. B., T. J. Hallam, and T. J. Rink. 1987. Single stretch-activated channels in vascular endothelial cells as mechanotrasducers? *Nature*. 325:811–813.

Lech, D., and R. Brent. 1995. *Escherichia coli*, media preparation and bacteriological tools. *In* Current Protocols in Molecular Biology, F. M. Ausubel, R. Brent, R. E. Kingston, D. D. Moore, J. G. Seidman, J. A. Smith, and K. Struhl, editors. John Wiley and Sons, Cambridge, MA. 1.1.1–1.1.4

Levina, N., S. Tötemeyer, N. R. Stokes, P. Louis, M. A. Jones, and I. R. Booth. 1999. Protection of *Escherichia coli* cells against extreme turgor by activation of MscS and MscL mechanosensitive channels: identification of genes required for MscS activity. *EMBO J.* 18:1730–1737.

Martinac, B., M. Buechner, A. H. Delcour, J. Adler, and C. Kung. 1987. Pressure-sensitive ion channel in *Escherichia coli. Proc. Nat. Acad. Sci. USA.* 84:2297–2301.

Moe, P. C., P. Blount, and C. Kung. 1998. Functional and structural conservation in the mechanosensitive channel MscL implicates elements crucial for mechanosensation. *Mol. Microbiol.* 28:583–592.

Nakamaru, Y., Y. Takahashi, T. Unemoto, and T. Nakamura. 1999. Mechanosensitive channel functions to alleviate the cell lysis of marine bacterium, *Vibrio alginolyticus*, by osmotic downshock. *FEBS Lett.* 444:170–172.

Ou, X., P. Blount, R. Hoffman, and C. Kung. 1998. One face of a transmembrane helix is crucial in mechanosensitive channel gating. *Proc. Nat. Acad. Sci. USA.* 95:11471–11475.

Sachs, F., and C. E. Morris. 1998. Mechanosensitive ion channels in nonspecialized cells. *Rev. Physiol. Biochem. Pharmacol.* 132:1–77.

Sackin, H. 1995. Mechanosensitive channels. *Ann. Rev. Physiol.* 57: 333–353.

Saint, N., J. J. Lacapère, L. Q. Gu, A. Ghazi, B. Martinac, and J. L. Rigaud. 1998. A hexameric transmembrane pore revealed by two-dimensional crystallization of the large mechanosensitive ion channel (MscL) of *Escherichia coli. J. Biol. Chem.* 273:14667–14670.

Sukharev, S. I., B. Martinac, V. Y. Arshavsky, and C. Kung. 1993. Two types of mechanosensitive channels in the *Escherichia coli* cell envelope: solubilization and functional reconstitution. *Biophys. J.* 65: 1–7.

Sukharev, S. I., P. Blount, B. Martinac, F. R. Blattner, and C. Kung. 1994. A large-conductance mechanosensitive channel in *E. coli* encoded by *mscL* alone. *Nature.* 368:265–268.

Sukharev, S. I., P. Blount, B. Martinac, and C. Kung. 1997. Mechanosensitive channels of *Escherichia coli*—the MscL gene, protein, and activities. *Ann. Rev. Physiol.* 59:633–657.

Sukharev, S. I., M. J. Schroeder, and D. R. McCaslin. 1999a. Re-examining the multimeric structure of the large conductance bacterial mechanosensitive channel, MscL. Biophysical Society Meeting, Baltimore, Maryland, USA. *Biophys. J.* 76:A138 (abstr.)

Sukharev, S. I., W. J. Sigrudson, C. Kung, and F. Sachs. 1999b. Energetic and spatial parameters for gating of the bacterial large conductance mechanosensitive channel, MscL. *J. Gen. Physiol.* 113:525–540.

Ubl, J., H. Murer, and H.-A. Kolb. 1988. Ion channels activated by osmotic and membrane stress in membranes of opossum kidney cells. *J. Memb. Biol.* 104:223–232.